

Long-range azimuthal correlations in proton-proton and proton-nucleus collisions from the incoherent scattering of partons

Guo-Liang Ma^a, Adam Bzdak^b

^aShanghai Institute of Applied Physics, Chinese Academy of Sciences, Shanghai 201800, China

^bRIKEN BNL Research Center, Brookhaven National Laboratory, Upton, NY 11973, USA

Abstract

We show that the incoherent elastic scattering of partons, as present in a multi-phase transport model (AMPT), with a modest parton-parton cross-section of $\sigma = 1.5 - 3$ mb, naturally explains the long-range two-particle azimuthal correlation as observed in proton-proton and proton-nucleus collisions at the Large Hadron Collider.

1. Introduction

Recent experimental observations of the long-range azimuthal correlations in high-multiplicity proton-proton (p+p) [1] and proton-nucleus (p+A) collisions [2–5] shed some new light on our understanding of *fireballs* created in such interactions.

The measured two-particle correlation function as a function of the pseudorapidity separation, $\Delta\eta = \eta_1 - \eta_2$, and the relative azimuthal angle, $\Delta\phi = \phi_1 - \phi_2$, of two particles demonstrates a great deal of similarity to that measured in peripheral heavy-ion collisions [6]. In particular, two particles separated by many units of pseudorapidity prefer to have similar azimuthal angles thus the two-particle correlation function is peaked at $\Delta\phi = 0$. Exactly the same phenomenon was observed in heavy-ion collisions where it is believed to originate from hydrodynamical evolution present in such interactions [7]. In this picture the initial anisotropic distribution of matter, characterized e.g. by ellipticity, is translated to the final momentum anisotropy with $\cos(2\Delta\phi)$ term (and higher harmonics) in the correlation function. However, the applicability of hydrodynamics to small systems, as the ones created in p+p and p+A interactions, is questionable and so far there is no consensus in this matter. Nevertheless, hydrodynamics¹ applied to p+p and p+A collisions results in qualitative and partly quantitative understanding of various sets of data [8–14]. On the other hand, the Color Glass Condensate [15], the effective description of low-x gluons

in the hadronic/nuclear wave function, results in equally good description of the two-particle correlation functions [16] (see also [17, 18] for a more qualitative discussion). The advantage of the CGC approach over hydrodynamics is its microscopic character and internal consistency. On the other hand, hydrodynamics naturally describes various sets of data for which the CGC predictions are often not clear. Moreover, hydrodynamics provides a solid intuitive understanding of the observed signal which is not the case for the CGC. To summarize, at present we have two competing languages² to understand small systems and it is crucial to establish the true origin of the long-range azimuthal correlation. Several observables and arguments [20–33] were recently put forward which hopefully can help to resolve this interesting issue.

In this paper, we calculate the two-particle density function, $N^{\text{pair}}(\Delta\eta, \Delta\phi)$, in p+p and p+Pb collisions assuming the incoherent elastic scattering of partons, as present in a multi-phase transport model (AMPT) [34]. This approach is simple and intuitive, and more importantly is closely related to quantum chromodynamics (QCD). The cascade model with the reasonable parton-parton cross-section, $\sigma = 1 - 10$ mb, was proved to be very successful in understanding many features of heavy-ion collision data, see e.g. [35–38]. This approach has one crucial advantage over hydrodynamics, namely, there is no need to assume local thermalization. So far such a calculation was not published and it is important to establish whether a simple incoherent scattering of partons with a reasonable partonic cross-section can generate the long-range struc-

Email addresses: glma@sinap.ac.cn (Guo-Liang Ma), abzdak@quark.phy.bnl.gov (Adam Bzdak)

¹It should be noted that the long-range rapidity structure is put by hand into hydrodynamic calculations.

²In Ref. [19] both physical pictures are argued to be rather connected.

ture in p+p and p+A two-particle correlation functions.³

Our main result is that the incoherent elastic scattering of partons, with a partonic cross-section of $\sigma = 1.5 - 3$ mb, naturally generates the long-range azimuthal correlation of charged particles both in p+p and p+A collisions. A near side peak at $\Delta\phi = 0$ grows with the growing number of produced particles due to the growing density of partons, and consequently the larger number of partonic scatterings. The p_T dependence of the near-side peak is also reproduced that is, the signal at $\Delta\phi = 0$ is best visible for $1 < p_T < 2$ GeV/c.

In the next section we give a brief introduction to the AMPT model. In Section 3 we present our results for the two-particle correlation functions in p+p and p+A collisions for various multiplicity and p_T bins. We finish our paper with comments in Section 4 and conclusions in Section 5.

2. Model

The AMPT model with string melting mechanism is employed in this work (for comparison we also show some results obtained in the default model). It is initialized with a spatial and momentum distribution of mini-jet partons and soft string excitations from the HIJING model [39]. The string melting mechanism converts all excited strings into quarks and antiquarks according to the flavor and spin structures of their valence quarks (in contrast to the default AMPT model, where only partons from minijets are present). The evolution of a quark-antiquark plasma⁴ is modeled by a simple parton cascade. At present, the parton cascade includes only two-body elastic scatterings with a cross-section obtained from the pQCD with a screening mass [40]. Clearly this is a simplified picture however, we believe it captures the main features of parton dynamics present at the early stage of a collision. The parton cascade is followed by the hadronization, where quarks are recombined into hadrons via a simple coalescence model. Finally dynamics of the subsequent hadronic matter is described by a relativistic transport model [41]. For more details on the AMPT model we refer the reader to Ref. [34]. The recent AMPT studies show that the partonic cross-section of 1.5 mb can describe many experimental observables at the LHC [36, 38, 42, 43]. In particular it was found that

³We note that the negative result was reported by the CMS Collaboration in Ref. [2]. Our results contradict their conclusion.

⁴In our context we only need partonic scatterings and the composition of the partonic matter is less important.

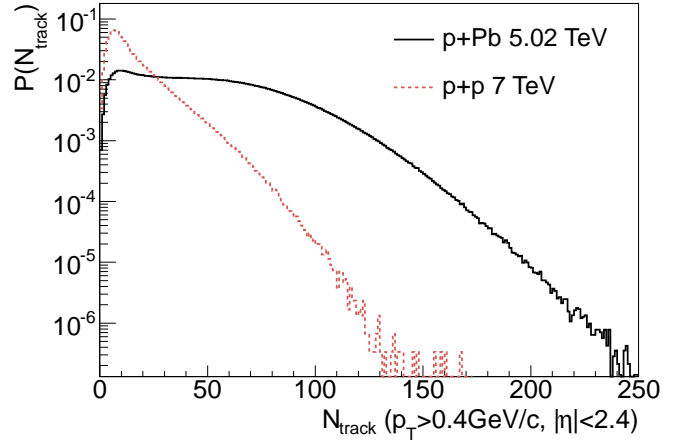


Figure 1: The multiplicity distribution calculated in AMPT, $P(N_{\text{track}})$, as a function of the number of produced particles, N_{track} , in p+p collisions at $\sqrt{s} = 7$ TeV, and p+Pb collisions at $\sqrt{s} = 5.02$ TeV for charged particles produced in $|\eta| < 2.4$ and $p_T > 0.4$ GeV/c.

the long-range azimuthal correlation can be produced by the parton scatterings in Pb+Pb collisions at $\sqrt{s} = 2.76$ TeV [44].

3. Results

To directly compare our results with the CMS data we select events with different values of the number of produced charged particles, N_{track} . In Figure 1 we present the multiplicity distributions, $P(N_{\text{track}})$, in p+p collisions at $\sqrt{s} = 7$ TeV and p+Pb interactions at $\sqrt{s} = 5.02$ TeV, for charged particles produced in $|\eta| < 2.4$ and $p_T > 0.4$ GeV/c. Both multiplicity distributions are in reasonable agreement with the CMS data⁵, see e.g. [45].

Before we present our main results it could be pedagogical to illustrate the initial parton distribution in the transverse plane in p+p and p+A collisions with $N_{\text{track}} > 110$. As seen in Figure 2 the initial size of a system in p+p is roughly a factor of 2 smaller than that in p+A. We checked that in a p+p collision partons are produced mainly in the overlap region of the two colliding protons, leading to a characteristic elliptical shape in a typical p+p event. In a p+A collision, the produced partons are localized in a few spots corresponding to the positions of the wounded nucleons [46].

In Fig. 3 we show the AMPT results for the two-particle density function in p+Pb collisions at $\sqrt{s} = 5.02$ TeV as a function of the relative azimuthal angle, $\Delta\phi = \phi_1 - \phi_2$, and the pseudorapidity separation, $\Delta\eta = \eta_1 - \eta_2$, for

⁵We do not compare directly with the CMS data since their $N_{\text{track}}^{\text{offline}}$ is not exactly our N_{track} .

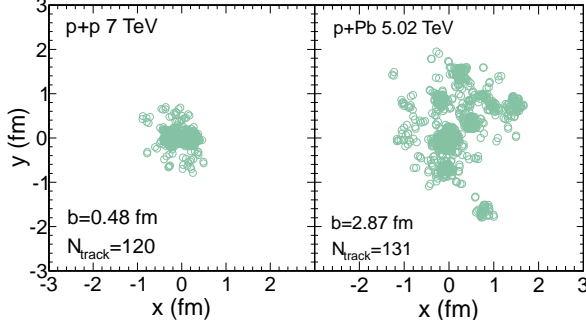


Figure 2: The initial parton distribution in a p+p collision (left panel) and a p+Pb collision (right panel) for two typical AMPT events (with string melting mechanism) with the number of produced charged particles, N_{track} , larger than 110 ($|\eta| < 2.4$, $p_T > 0.4$ GeV/c). Here b is the impact parameter.

events with $N_{\text{track}} < 35$ (left) and $N_{\text{track}} > 110$ (right). In this plot we take the pairs of charged particles with $1 < p_T < 3$ GeV/c. In qualitative agreement with the experimental data, the long-range near-side structure is absent for events with $N_{\text{track}} < 35$ and is clearly visible in events with $N_{\text{track}} > 110$.

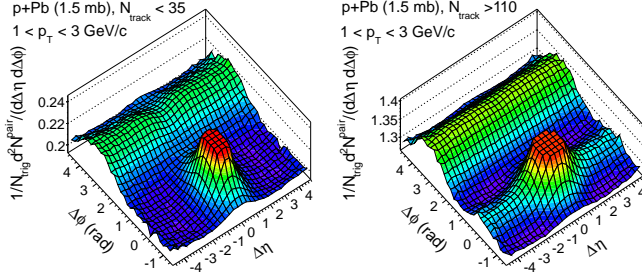


Figure 3: The AMPT two-particle density function in p+Pb collisions at $\sqrt{s} = 5.02$ TeV for low- (left) and high- (right) multiplicity events. The long-range near-side structure in pseudorapidity is clearly visible for high-multiplicity events.

To compare directly with the data, in Fig. 4 we present the two-particle distribution functions for p+Pb collisions at $\sqrt{s} = 5.02$ TeV and p+p at $\sqrt{s} = 7$ TeV, as a function of the relative azimuthal angle $\Delta\phi$ and averaged over pseudorapidity region $2 < |\Delta\eta| < 4$

$$\frac{1}{N_{\text{trig}}} \frac{d^2 N^{\text{pair}}}{d\Delta\phi} = \frac{1}{4} \int_{2 < |\Delta\eta| < 4} \frac{1}{N_{\text{trig}}} \frac{d^2 N^{\text{pair}}}{d\Delta\phi d\Delta\eta} d\Delta\eta, \quad (1)$$

for various ranges of N_{track} and different p_T bins. Following the experimental procedure the zero-yield-at-minimum (ZYAM) method is implemented to remove a constant background, C_{ZYAM} . In this calculation we take the partonic cross-section to be $\sigma = 1.5$ mb. The AMPT results (solid and dashed curves) are in very good agreement with the CMS data (full and open circles) for the

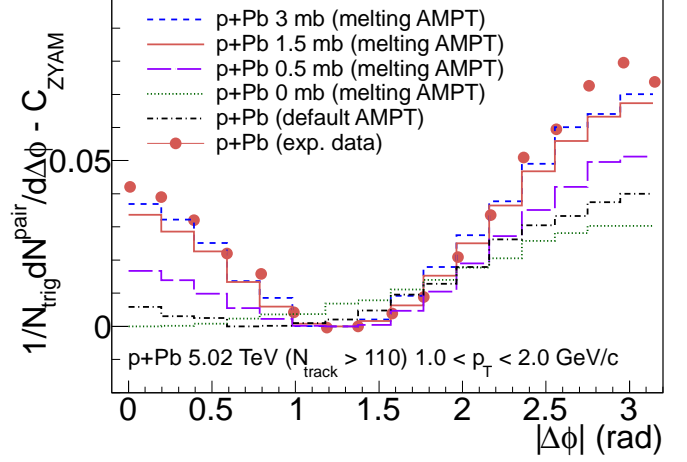


Figure 5: Distribution of pairs for various values of the partonic cross-section, σ , in p+Pb collisions at $\sqrt{s} = 5.02$ TeV as a function of the relative azimuthal angle $\Delta\phi$ averaged over $2 < |\Delta\eta| < 4$ for $N_{\text{track}} > 110$ and $1 < p_T < 2$ GeV/c. Our results (curves) from different AMPT model settings are compared with the CMS data (points). In the default AMPT model only few partons from minijets interact which is not sufficient to produce a sizable signal. In the string melting version all soft strings are converted into partons.

near-side peak, $\Delta\phi \approx 0$. The agreement with the away-side peak, $\Delta\phi \approx \pi$, is less impressive however, this region is heavily populated by jets which are of lesser interest in the present investigation. It is worth noticing that at the same N_{track} bin, the signal at $\Delta\phi = 0$ in p+p collisions is noticeably smaller than that in p+A interactions. This feature agrees very well with the CMS data.

In Figure 5 we present the results for p+Pb collisions calculated in the AMPT model with various values of $\sigma = 0, 0.5, 1.5$, and 3 mb. We also show the result of the default AMPT model, where only partons from minijets interact and all soft strings decay independently into particles. In this scenario the number of interacting partons is not sufficiently high to produce a visible effect. On the contrary, in the string melting scenario (in which all initial soft strings melt into partons) the number of interacting partons is significantly larger, roughly a factor of 5, thus allowing to obtain a sizable signal. As seen in Figure 5 the strength of the signal gradually increases with growing σ and, as expected, the signal vanishes completely for $\sigma = 0$ mb. It clearly demonstrates that in the AMPT model partonic scatterings are directly responsible for the signal at $\Delta\phi = 0$, as observed in Figures 4 and 5.

In the last part of the paper we address the problem of the p_T particle spectra. The measured p_T distributions evolve towards higher p_T with an increasing number of produced particles [47]. In principle this feature should be present in the AMPT model with the string melting mech-

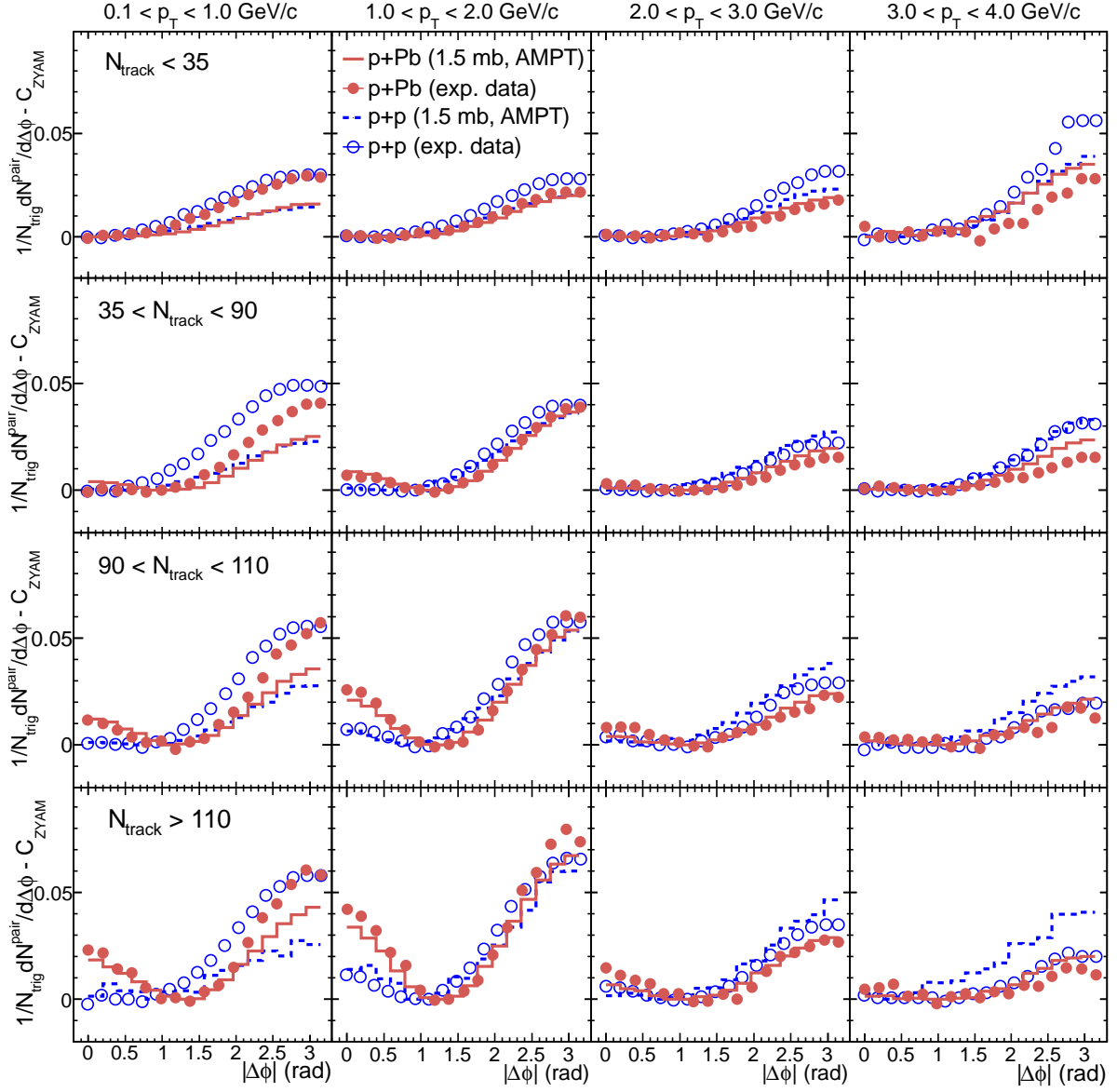


Figure 4: Distribution of pairs in p+p collisions at $\sqrt{s} = 7$ TeV and p+Pb collisions at $\sqrt{s} = 5.02$ TeV as a function of the relative azimuthal angle $\Delta\phi$ averaged over $2 < |\Delta\eta| < 4$ in different p_T and N_{track} bins. Our results (solid and dashed curves) based on the AMPT model (with string melting, $\sigma = 1.5$ mb) are compared to the CMS data (full and open circles).

anism owing to the frequent parton-parton scatterings. However, in our model the hadronization mechanism is rather crude (a simple coalescence) thus we should not expect the model to be particularly successful in describing the spectra (in contrast to the studied long-range rapidity correlation which presence or absence is independent on the particular mechanism of hadronization). Nevertheless, it is interesting to investigate whether the AMPT model can approximately reproduce the trends observed in the data. In Fig. 6 we present the p_T distributions of produced pions, kaons and protons in p+Pb collisions for several centrality classes. The model, despite its simplicity, reproduces the CMS data [47] within the accuracy of 20%. The calculated spectra shift towards higher p_t with an increasing number of produced particles, N_{track} , as best visible in the rightmost plot (p+p̄).

4. Comments

It is worth noticing that the incoherent scattering of partons with basically one essential parameter, $\sigma = 1.5 - 3$ mb, allows to capture the main features of the p+p and p+Pb data for all measured multiplicities and the transverse momenta. This may be contrasted with the CGC framework [16] where the saturation scale is fitted separately for each multiplicity and the colliding system.

The presence of the near-side peak in our results originates from the parton scatterings at the early stage of a collision, see Figure 5. Obviously the lifetime, τ , of the partonic stage increases with increasing number of initial partons, and consequently with N_{track} . We checked that in p+Pb collisions $\tau \sim N_{\text{track}}^\alpha$ with $\alpha \sim 1/2$ and for $N_{\text{track}} = 50, 100, 200$ the lifetime $\tau \approx 1, 1.4, 1.7$ fm, respectively. In p+p collisions τ grows slowly from $\tau \approx 0.6$ fm for $N_{\text{track}} = 10$ to $\tau \approx 0.8$ fm for $N_{\text{track}} = 100$. Our results indicate that for small and rapidly expanding systems there is enough time for multiple parton scatterings which can translate the initial anisotropy of produced matter into the final momentum anisotropy.

There are several problems in our approach that require further studies. For example only two-to-two elastic parton scatterings are included and higher order processes might become important at high densities. For a complete discussion of various problems in the partonic stage of the AMPT model we refer the reader to Section VII in Ref. [34].

A transport model calculations reported in Ref. [48] suggest that a parton-parton cross-section of the order of 50 mb is needed to generate a sizable elliptic flow in A+A collisions. However, in the AMPT model a cross-section

of the order of 1.5–5 mb is enough to reproduce the A+A data. It would be interesting to understand the origin of this contradiction.⁶

We would like to emphasize that our goal was not to fit precisely the data. Our objective was to check if a minimal implementation of partonic scatterings, with a reasonable cross-section, can roughly reproduce the experimental data for p+p and p+Pb collisions. As seen in Figure 5, the agreement with the experimental data is surprisingly good, suggesting that various shortcomings present in our approach are not very important.

It would be interesting to extend our discussion for peripheral Pb+Pb collisions. We leave this problem for a separate investigation. Also the detailed discussion of the elliptic and triangular [49] Fourier coefficients will be reported elsewhere.

5. Conclusions

In summary, we demonstrated that the incoherent scattering of partons in the early stage of p+p and p+A collisions is sufficient to understand the near-side azimuthal correlation of particles separated by a large gap in pseudorapidity. Using the multi-phase transport model (AMPT with string melting), with a parton-parton cross-section of 1.5 mb, we calculated the two-particle correlation function as a function of $\Delta\eta$ and $\Delta\phi$. The main trends observed in the data were successfully reproduced. The near-side peak at $\Delta\phi = 0$ is gradually growing with the number of produced particles owing to the growing density of partons. This in consequence leads to more frequent parton-parton scatterings. Moreover, the signal is best visible in the transverse momentum range $1 < p_T < 2$ GeV/c, being in agreement with the CMS data.

In the default AMPT model, where only partons from minijets interact and soft strings decay independently into particles, the number of interacting partons is not sufficient to produce a visible signal.

Our study indicates that even in a very small system, as the one created in a p+p collision, there is enough time for partonic scatterings before the system becomes dilute. These scatterings translate the initial anisotropy of matter into the final momentum anisotropy, leading to the $\cos(2\Delta\phi)$ term (and higher harmonics) in the azimuthal correlation function.

In this paper we focused solely on the main features of the two-particle correlation function. Calculations of the elliptic and triangular Fourier coefficients in p+p, p+A

⁶We thank D. Molnar and P. Petreczky for comments on this point.

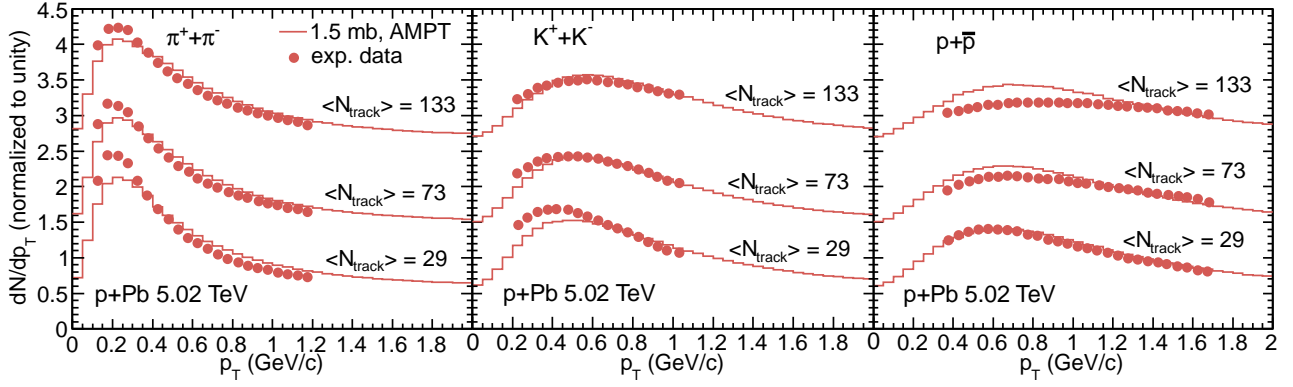


Figure 6: The transverse momentum spectra (normalized to unity) in $|y| < 1$ of produced pions, kaons and protons in p+Pb collisions at $\sqrt{s} = 5.02$ TeV for three different centrality classes. The AMPT model (string melting) results are compared to the CMS data (full points). For better visibility, the results for $\langle N_{\text{track}} \rangle_{p_T > 0.4 \text{ GeV}/c} = 29, 73$ and 133 are shifted vertically by 0.6, 1.5 and 2.7 units, respectively.

and peripheral A+A collisions are left for a separate investigation.

Acknowledgments

We thank Wei Li for clarifications regarding the CMS results. Discussions with L. McLerran, V. Skokov and R. Venugopalan are appreciated.

G.-L.M. is supported by the Major State Basic Research Development Program in China under Contract No. 2014CB845404, the NSFC of China under Projects No. 11175232, No. 11035009, and No. 11375251, the Knowledge Innovation Program of CAS under Grant No. KJCX2-EW-N01, CCNU-QLPL Innovation Fund under Grant No. QLPL2011P01, and the “Shanghai Pujiang Program” under Grant No. 13PJ1410600.

A.B. is supported through the RIKEN-BNL Research Center and the grant No. UMO-2013/09/B/ST2/00497.

References

- [1] V. Khachatryan *et al.* [CMS Collaboration], JHEP **1009**, 091 (2010) [arXiv:1009.4122 [hep-ex]].
- [2] S. Chatrchyan *et al.* [CMS Collaboration], Phys. Lett. B **718** (2013) 795 [arXiv:1210.5482 [nucl-ex]].
- [3] B. Abelev *et al.* [ALICE Collaboration], Phys. Lett. B **719**, 29 (2013) [arXiv:1212.2001].
- [4] G. Aad *et al.* [ATLAS Collaboration], Phys. Rev. Lett. **110**, 182302 (2013) [arXiv:1212.5198 [hep-ex]].
- [5] A. Adare *et al.* [PHENIX Collaboration], Phys. Rev. Lett. **111**, 212301 (2013) [arXiv:1303.1794 [nucl-ex]].
- [6] S. Chatrchyan *et al.* [CMS Collaboration], Phys. Lett. B **724**, 213 (2013) [arXiv:1305.0609 [nucl-ex]].
- [7] W. Florkowski, Phenomenology of Ultra-Relativistic Heavy-Ion Collisions (World Scientific Publishing Company, Singapore, 2010).
- [8] P. Bozek, Phys. Rev. C **85**, 014911 (2012) [arXiv:1112.0915 [hep-ph]].
- [9] E. Shuryak and I. Zahed, Phys. Rev. C **88**, 044915 (2013) [arXiv:1301.4470 [hep-ph]].
- [10] P. Bozek and W. Broniowski, Phys. Rev. C **88**, 014903 (2013) [arXiv:1304.3044 [nucl-th]].
- [11] A. Bzdak, B. Schenke, P. Tribedy and R. Venugopalan, Phys. Rev. C **87**, 064906 (2013) [arXiv:1304.3403 [nucl-th]].
- [12] G. -Y. Qin and B. Mueller, Phys. Rev. C **89**, 044902 (2014) [arXiv:1306.3439 [nucl-th]].
- [13] K. Werner, B. Guiot, I. Karpenko and T. Pierog, Phys. Rev. C **89**, 064903 (2014) [arXiv:1312.1233 [nucl-th]].
- [14] P. Bozek, W. Broniowski and G. Torrieri, Phys. Rev. Lett. **111**, 172303 (2013) [arXiv:1307.5060 [nucl-th]].
- [15] F. Gelis, E. Iancu, J. Jalilian-Marian and R. Venugopalan, Ann. Rev. Nucl. Part. Sci. **60**, 463 (2010) [arXiv:1002.0333 [hep-ph]].
- [16] K. Dusling and R. Venugopalan, Phys. Rev. D **87**, 094034 (2013) [arXiv:1302.7018 [hep-ph]].
- [17] Y. V. Kovchegov and D. E. Wertheim, Nucl. Phys. A **906**, 50 (2013) [arXiv:1212.1195].
- [18] A. Kovner and M. Lublinsky, Int. J. Mod. Phys. E **22**, 1330001 (2013) [arXiv:1211.1928 [hep-ph]].
- [19] T. Epelbaum and F. Gelis, Phys. Rev. Lett. **111**, 232301 (2013) [arXiv:1307.2214 [hep-ph]].
- [20] A. Bzdak and V. Skokov, Phys. Rev. Lett. **111**, 182301 (2013) [arXiv:1307.6168 [hep-ph]].
- [21] P. Bozek, A. Bzdak and V. Skokov, Phys. Lett. B **728**, 662 (2014) [arXiv:1309.7358 [hep-ph]].
- [22] C. E. Coleman-Smith and B. Mueller, Phys. Rev. D **89**, 025019 (2014) [arXiv:1307.5911 [hep-ph]].
- [23] J. D. Bjorken, S. J. Brodsky and A. Scharff Goldhaber, Phys. Lett. B **726**, 344 (2013) [arXiv:1308.1435 [hep-ph]].
- [24] L. McLerran, M. Praszalowicz and B. Schenke, Nucl. Phys. A **916**, 210 (2013) [arXiv:1306.2350 [hep-ph]].
- [25] A. H. Rezaeian, Phys. Lett. B **727**, 218 (2013) [arXiv:1308.4736 [hep-ph]].
- [26] G. Basar and D. Teaney, arXiv:1312.6770 [nucl-th].
- [27] A. Bzdak, P. Bozek and L. McLerran, Nucl. Phys. A **927**, 15 (2014) [arXiv:1311.7325 [hep-ph]].
- [28] L. Yan and J. Y. Ollitrault, Phys. Rev. Lett. **112**, 082301 (2014) [arXiv:1312.6555 [nucl-th]].
- [29] A. Bzdak and V. Skokov, arXiv:1312.7349 [hep-ph].
- [30] V. P. Konchakovski, W. Cassing and V. D. Toneev, arXiv:1401.4409 [nucl-th].

- [31] A. Bzdak and V. Skokov, Phys. Lett. B **726**, 408 (2013) [arXiv:1306.5442 [nucl-th]].
- [32] A. M. Sickles, Phys. Lett. B **731**, 51 (2014) [arXiv:1309.6924 [nucl-th]].
- [33] J. Noronha and A. Dumitru, Phys. Rev. D **89**, 094008 (2014) [arXiv:1401.4467 [hep-ph]].
- [34] Z. -W. Lin, C. M. Ko, B. -A. Li, B. Zhang and S. Pal, Phys. Rev. C **72**, 064901 (2005) [nucl-th/0411110].
- [35] G. -L. Ma and X. -N. Wang, Phys. Rev. Lett. **106**, 162301 (2011) [arXiv:1011.5249 [nucl-th]].
- [36] J. Xu and C. M. Ko, Phys. Rev. C **83**, 034904 (2011) [arXiv:1101.2231 [nucl-th]].
- [37] D. Solanki, P. Sorensen, S. Basu, R. Raniwala and T. K. Nayak, Phys. Lett. B **720**, 352 (2013) [arXiv:1210.0512 [nucl-ex]].
- [38] G. -L. Ma, Phys. Rev. C **87**, 064901 (2013) [arXiv:1304.2841 [nucl-th]].
- [39] X. -N. Wang and M. Gyulassy, Phys. Rev. D **44**, 3501 (1991).
- [40] B. Zhang, Comput. Phys. Commun. **109**, 193 (1998) [nucl-th/9709009].
- [41] B. -A. Li and C. M. Ko, Phys. Rev. C **52**, 2037 (1995) [nucl-th/9505016].
- [42] J. Xu and C. M. Ko, Phys. Rev. C **84**, 014903 (2011) [arXiv:1103.5187 [nucl-th]].
- [43] G. -L. Ma, Phys. Lett. B **724**, 278 (2013) [arXiv:1302.5873 [nucl-th]].
- [44] J. Xu and C. M. Ko, Phys. Rev. C **84**, 044907 (2011) [arXiv:1108.0717 [nucl-th]].
- [45] W. Li for the CMS Collaboration, talk at the pA Physics Workshop at MIT, Cambridge, MA USA, 2013.
- [46] A. Bialas, M. Bleszynski and W. Czyz, Nucl. Phys. B **111**, 461 (1976).
- [47] S. Chatrchyan *et al.* [CMS Collaboration], Eur. Phys. J. C **74**, 2847 (2014) [arXiv:1307.3442 [hep-ex]].
- [48] D. Molnar and P. Huovinen, Phys. Rev. Lett. **94**, 012302 (2005) [nucl-th/0404065].
- [49] B. Alver and G. Roland, Phys. Rev. C **81**, 054905 (2010) [Erratum-ibid. C **82**, 039903 (2010)] [arXiv:1003.0194 [nucl-th]].